International Journal on
"Technical and Physical Problems of Engineering"
(IJTPE)
Published by International Organization of IOTPE

ISSN 2077-3528
IJTPE Journal
www.iotpe.com
ijtpe@iotpe.com

March 2014 | Issue 18 | Volume 6 | Number 1 | Pages 114-124

A COMPARATIVE STUDY OF ACTIVE AND REACTIVE POWER CONTROLLER FOR A DOUBLY FED INDUCTION GENERATOR (DFIG) USING DPC AND FOC STRATEGIES

M. Ghorbani B. Mozaffari S. Soleymani

Department of Electrical Engineering, Science and Research Branch, Islamic Azad University, Tehran, Iran
ghorbani_m7@yahoo.com, mozafari_babak@yahoo.com, soodabeh_soleymani@yahoo.com

Abstract- In this research control of active and reactive power of a double-fed induction generator have been surveyed by using two control method based on field oriented control and direct power control and then the results have been compared with each other in different scenarios. The simulation has been accomplished by PSCAD/EMTDC software and the generator rated power is 2 MW. First simulation section shows the performance of mentioned strategy in different rotor speed condition including super-synchronous, synchronous and sub-synchronous. In the second section the value of stator resistance, applied in simulation, have been allocated 70% and 130% of the rated value to determine the robustness of methods despite error in stator resistance value estimation. In the next step, double-fed induction generator in torque control mode is surveyed and obtained results show that direct power control, despite its simplicity, has faster dynamic reaction and good performance in different conditions. In the direct power control method, the stator resistance is needed as an input parameter, which usually is estimated. Results show that the error caused by estimation of this parameter, do not decrease the effectiveness of this method.

Keywords: Wind Turbine, Double-Fed Induction Generator, Field Oriented Control, Direct Power Control, Voltage Source Converter.

I. INTRODUCTION

The wind turbines are classified to fixed speed and variable speed. In the fixed speed concept, the generator connected to power network directly by converter and power electronic tools is not used for adjusting the speed of generator, the speed changes range is very low and its limitations is about 1% to 5% of rated speed. The variable speed wind turbines are divided to wind turbines with Double-Fed Induction Generators (DFIG) and the ones with fully rated converter which is based on synchronous or induction generator. These generators separate rotation speed from network frequency by power electronic tools.

The wind turbine with double-fed induction generator is the most common, which its stator connected to network directly and rotor is connected to network by the variable frequency power converters that are made of two IGBT Voltage Source Converter (VSC) which are connected to each other by a DC-link. The structure of DFIG based wind turbine scheme has been shown in Figure 1. The induction generator is including slip rings for creating the current path to the rotor.

In addition, variable speed operation is obtained by injecting a controllable voltage into the rotor at desired slip frequency. When generator works in super-synchronous speed, power will be delivered from the rotor through the converters to the network and when the generator operates in sub-synchronous mode, the rotor will absorb power from the network [1-3]. These two operation modes are illustrated in Figure 2. In variable speed wind turbine with fully rated converter, synchronous generator, or induction generator are used in system which converters are Interface of stator and network.

In the DFIG based wind generator, low capacity converter (about 30% of generator rated power) is used which has less power losses and consequently lower converter cost. These are the characteristics of DFIG, which cause its priority to generators with fully rated converter. Also comparing with fixed speed generators, DFIG can be operated in generation mode at range of 20% to 30% synchronous speed that enables power control [4].

In recent decades, different strategies for controlling the active and reactive power flow between double-fed induction generator and network have been offered, one of the most important control methods on rotor side converter that has attracted special consideration in recent decade, is Field oriented control (FOC) and new method of direct power control (DPC).

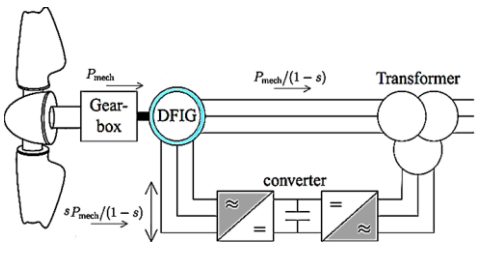

Figure 1. Schematic diagram of the DFIG-based wind energy generation system [3]

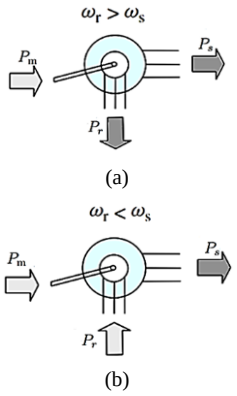

Figure 2. (a) Super-synchronous and, (b) sub-synchronous operation of the DFIG wind turbine

The first method is based on controlling the rotor current vector by using the rotating (d-q) transformation that i_q and i_d of control the active an reactive stator respectively. This method needs detailed parameters of the machine such as rotor and stator resistance and inductance and the mutual inductance. In addition, due to existence of current control loops and PI controllers, for stability guaranty and having proper response in all states of system performance, controller should be adjusted precisely [5-7].

Direct active and reactive power control strategy, is presented based on stator flux estimation and assuming constant stator voltage frequency, estimating accuracy of the stator flux is guaranteed. In this method, switching the rotor side converter is performed with optimal switching table by using the estimated stator flux position and error of active and reactive power. Therefore, this control system is very simple and effect of machine parameters on system performance is lower [8-11].

Choosing proper control method that increases the statical and dynamical performance is very important. Considering that for controlling most of these generators, traditional control methods, among which One of the most common is the Field Oriented Control (FOC), still is being used, studies for surveying advantages and disadvantage of FOC and DPC is essential for determining which methods has a better performance in different condition of the system.

This paper investigates and studies the mentioned strategies ability in different scenarios including performance of DFIG in different rotor speed condition that consist of super-synchronous, synchronous and sub-synchronous, change in applied stator resistance value in simulation, as 70% and 130% rated value for evaluating the ability of mentioned methods and finally surveying the performance of DFIG in torque mode.

The main consideration in this article is the rotor side converter and control strategy of network side converter has been done by using of presented strategy in [5]. For fixing the DC-link voltage and simulation of the rotor side converter control system has been implemented by FOC and DPC methods and their dynamical behavior in steady state are compared with each other.

II. CONTROL OF NETWORK SIDE CONVERTER

Therefore, as mentioned in introduction, task of network side converter is controlling the DC-link voltage in a fix value without considering the rotor power-flow direction. For this converter, the vector control method has been used, in which d-axis of reference frame aligned along with stator voltage. Figure 3 shows the scheme of network side converter. The value of $V_{a,b,c}$ of the Figure 3 is the same as below equation [7]:

$$\begin{bmatrix} v_a \\ v_b \\ v_c \end{bmatrix} = R\begin{bmatrix} i_a \\ i_b \\ i_c \end{bmatrix} + L\frac{d}{dt}\begin{bmatrix} i_a \\ i_b \\ i_c \end{bmatrix} + \begin{bmatrix} v_{a1} \\ v_{b1} \\ v_{c1} \end{bmatrix} \tag{1}$$

Equation (1) transformed to dq synchronous reference frame by network voltage vector angular velocity, ω_e, and changes the same as below so that the voltage is converted from sinusoidal signal to DC [5].

$$\begin{cases} v_d = Ri_d + L\dfrac{di_d}{dt} - \omega_e L i_q + v_{d1} \\ v_q = Ri_q + L\dfrac{di_q}{dt} - \omega_e L i_q + v_{q1} \end{cases} \tag{2}$$

Position of network voltage angle, which is quantities conversion angle to synchronous reference frame, is accelerated by below equation [13]:

$$\theta_e = \int \omega_e dt = \tan^{-1}\frac{v_\beta}{v_\alpha} \tag{3}$$

where, v_β and v_α are voltage components in stationary frame. And also active and reactive power equations are the same as below [13]:

$$\begin{cases} P = 3\left(v_d i_d + v_q i_q\right) \\ Q = 3\left(v_d i_q + v_q i_d\right) \end{cases} \tag{4}$$

Considering that d axis and synchronous reference frame is aligned to position of network voltage vector (θ_e), the value of v_q will be zero and the value of v_d is equal with network voltage which is a fix amount. Consequently, according to Equation (4), active and reactive power are proportionated with the i_d and i_q, respectively and Enables the power flow control between network and converter. Neglecting harmonics caused by switching and coil resistance and converter losses, we will have [5]:

$$\begin{cases} Ei_{l1} = 3v_d i_d \\ v_d = \dfrac{m_1}{2\sqrt{2}}E \\ i_{l1} = \dfrac{3}{2\sqrt{2}}m_1 i_d \\ C\dfrac{dE}{dt} = i_{l1} - i_{l2} \end{cases} \tag{5}$$

It is clear from above equations that DC-link voltage can be controlled by i_d. In addition, reference of i_q is determined based on reactive power flow. Figure 4 shows a scheme of the network-side converter control system. By using the Equation (2), parameters of current control loops are determined the same as Equation (6).

$$F(s) = \frac{i_d(s)}{v'_d(s)} = \frac{i_q(s)}{v'_q(s)} = \frac{1}{Ls+R} \tag{6}$$

In other word $v_{q,d}$ is produced with crossing the difference between the measured and reference values of the $i_{d,q}$ from the PI controller, and the reference values of the applied voltage to the modulator is produced by the following equation:

$$\begin{cases} v_{d1}^{*} = -v'_{d} + \left(\omega_e L i_q + v_d\right) \\ v_{q1}^{*} = -v'_{q} - \left(\omega_e L i_d\right) \end{cases} \quad (7)$$

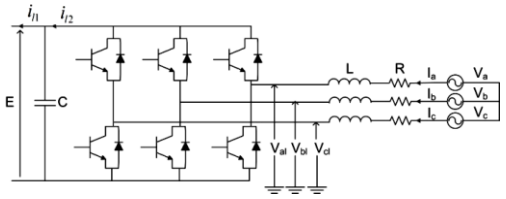

Figure 3. Grid side converter configuration [5]

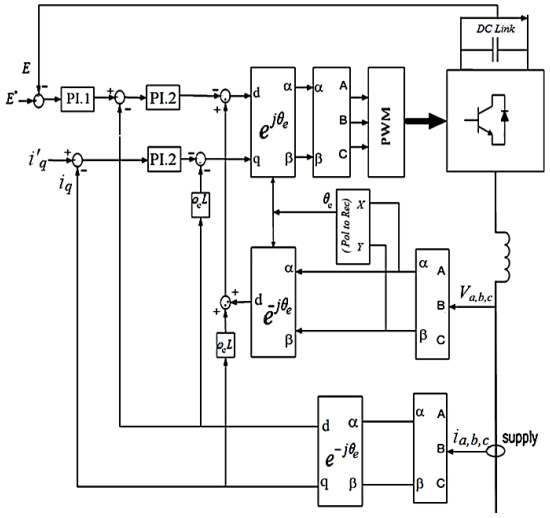

Figure 4. Schematic of the vector-control structure for grid side converter [4]

III. CONTROL OF ROTOR SIDE CONVERTER

During recent decades, different strategies for controlling the active and reactive power flow between double-fed induction generator and network have been offered. One of the most important control method applied on rotor side converter that has attracted special consideration is field oriented control method and direct power control, which the accuracy of performance in this methods is surveyed and the results have been compared with each other in different scenarios.

A. Active and Reactive Power Control by FOC Strategy

Field oriented control technique is used as a commonly known method for controlling the DFIG in different references. In this method DFIG has been surveyed in the synchronous reference frame, in which *d* axis of reference frame is aligned with stator flux vector that rotates by synchronous speed and q axis is conformed to stator voltage vector. This technique due to internal current control loops shows good statical and dynamical performance. Current of rotor has been separated to two perpendicular axis, d and q, in reference frame.

The q-axis current component is used for active power control, torque, or speed while the d current component is used for reactive power control or terminal voltage. Active and reactive power of stator is controllable by adjusting the current and voltage of rotor. Therefore, stator active and reactive power control is implemented on rotor side converter. In this strategy, by using the vector control, DFIG power control is performed [5-7]. Under stator-flux orientation, the relationship between the d-q axis voltages, currents, and fluxes may be written as [5]:

$$\begin{aligned} &\psi_s = \psi_{ds} = L_o i_{ms} = L_s i_{ds} + L_o i_{dr} \\ &\psi_{dr} = \frac{L_o^2}{L_s} i_{ms} + \sigma L_r i_{dr} \\ &\psi_{qr} = \sigma L_r i_{qr} \\ &i_{qs} = -\frac{L_o}{L_s} i_{qr} \end{aligned} \quad (8)$$

$$v_{dr} = R_r i_{dr} + \sigma L_r \frac{di_{dr}}{dt} - \omega_{slip} \sigma L_r i_{qr}$$

$$v_{qr} = R_r i_{qr} + \sigma L_r \frac{di_{qr}}{dt} + \omega_{slip} \left(L_m i_{ms} + \sigma L_r i_{dr}\right)$$

$$P = -3\frac{P}{2} \omega_e L_m i_{ms} i_{qr}$$

where, $\sigma = \left(L_o^2 / L_s L_r\right)$ and $L_m = \left(L_o^2 / L_s\right)$ and $\omega_{slip} = \omega_e - \omega_r$.

An essential thing for doing this process is controlling the measurement of stator and rotor current, stator voltage and position of rotor. Whereas, the stator is connected to network, magnetizing current i_{ms} can be supposed constant. Angle of stator flux is estimated using the following equation [5]:

$$\begin{cases} \psi_{\alpha s} = \int \left(v_{\alpha s} - R_s i_{\alpha s}\right) dt \\ \psi_{\beta s} = \int \left(v_{\beta s} - R_s i_{\beta s}\right) dt \\ \theta_s = \tan^{-1}\left(\psi_{\beta s} / \psi_{\alpha s}\right) \end{cases} \quad (9)$$

where, θ_s is the position of stator flux vector according to Equation (10), active power is proper with i_{qr} and can be adjusted by v_{qr}. In addition, reactive power has direct relation with i_{dr} and is controlled by v_{dr}.

Both references of q-axis and d-axis current component are obtained with crossing the difference between the measured value and reference value of the active and reactive power (respectively) from the PI controller. Figure 5 shows control system of rotor side converter with control strategy based on FOC. From equation of rotor voltage in Equation (8), we have:

$$\begin{cases} v'_{dr} = R_r i_{dr} + \sigma L_r \dfrac{di_{dr}}{dt} \\ v'_{qr} = R_r i_{qr} + \sigma L_r \dfrac{di_{qr}}{dt} \end{cases} \quad (10)$$

In this control strategy, difference of measured i_{dr} and i_{qr} from their reference values is calculated and are processed by PI controllers and according to Equations (8) and (10), for obtaining rotor voltages reference (v^*_{qr}, v^*_{dr}), values of $\omega_{slip}\left(L_m i_{ms} + \sigma L_r i_{dr}\right)$ and $-\omega_{slip}\sigma L_r i_{qr}$ should be added to v'_{qr} and v'_{dr}, respectively.

B. Control of Active and Reactive Power by DPC

Equivalent circuit of DFIG in rotor reference frame, which rotates with ω_r speed, is shown in Figure 6 and also relationship between stator and rotor flux in stationary and rotor reference frames is shown in Figure 7.

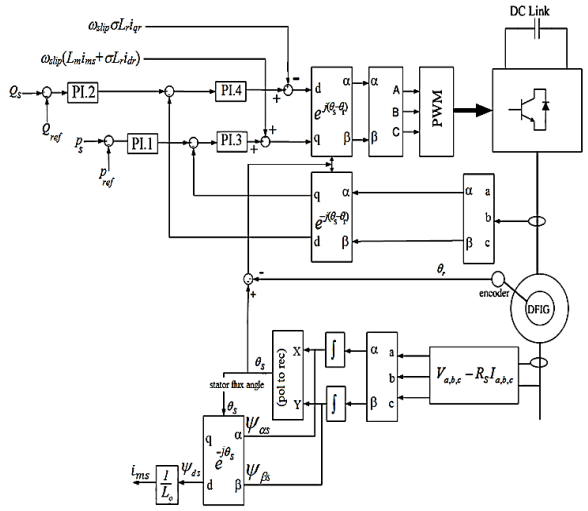

Figure 5. Schematic of FOC implementation for rotor side converter [5]

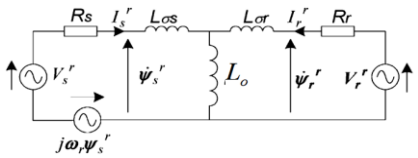

Figure 6. DFIG equivalent circuit in the rotor reference frame [8]

According to Figure 6, stator and rotor flux linkage vectors can be expressed as below:

$$\begin{cases}\psi_s^r = L_s I_s^r + L_o I_r^r \\ \psi_r^r = L_r I_r^r + L_o I_s^r\end{cases} \tag{11}$$

According to Equation (11), stator current is calculated as Equation (12):

$$I_s^r = \frac{L_r\psi_s^r - L_o\psi_r^r}{L_s L_r - L_o^2} = \frac{\psi_s^r}{\sigma L_s} - \frac{L_o\psi_r^r}{\sigma L_s L_r} \tag{12}$$

where, $\sigma = \left(L_o^2 / L_s L_r\right)$ is leakage coefficient.

From Figure 6 stator voltage vector is determined as below:

$$v_s^r = R_s I_s^r + \dot{\psi}_s^r + j\omega_r\psi_s^r \tag{13}$$

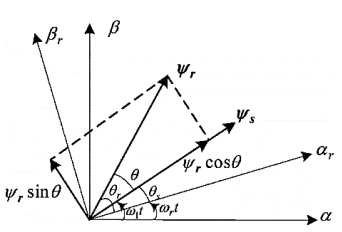

Figure 7. Stator and rotor flux linkage vectors in stationary and rotor reference frames [12]

The stator active power input from the network, neglecting stator copper loss, is expressed as below [10]:

$$P_s = \frac{3}{2}v_s^r I_s^r = \frac{3}{2}\left(\dot{\psi}_s^r + j\omega_r\psi_s^r\right)I_s^r \tag{14}$$

Similarly stator reactive power output to the network is expressed as below:

$$Q_s = -\frac{3}{2}v_s^r \times I_s^r = -\frac{3}{2}\left(\dot{\psi}_s^r + j\omega_r\psi_s^r\right)\times I_s^r \tag{15}$$

In considering Figure 7 stator and rotor flux in rotor reference frame can be expressed as below:

$$\psi_r^r = |\psi_r^r| e^{j\theta_r} \tag{16}$$

$$\psi_s^r = |\psi_s^r| e^{j\theta_s} \tag{17}$$

$$\psi_s^r = \psi_s^s e^{-j\omega_r t} \tag{18}$$

$$\dot{\theta}_s = \omega_1 - \omega_r \tag{19}$$

Stator flux in stationary reference frame is determined as below:

$$\psi_s^s = \int \left(v_s^s - R_s I_s^s\right)dt \tag{20}$$

Neglecting the stator winding resistance and by assumption that connected network to stator is stable and rotor speed during sampling does not change (due to high inertia of wind turbine) we will have [8]:

$$|\psi_s^r| = |\psi_s^s e^{-j\omega_r t}| = |\int v_s^s dt| = const\ ant \Rightarrow \frac{d|\psi_s^r|}{dt} = 0 \tag{21}$$

By differentiation of the Equation (16) and by using the Equation (17) we will have:

$$\dot{\psi}_s^r = |\psi_s^r| j\dot{\theta}_s e^{j\theta_s} = j\left(\omega_1 - \omega_r\right)\psi_s^r \tag{22}$$

By substituting of Equations (12) and (22) in Equation (14) and (15), for active and reactive powers of stator [8]:

$$P_s = -\frac{3}{2}\frac{L_o}{\sigma L_s L_r}\omega_1 |\psi_s^r||\psi_r^r|\sin\theta \tag{23}$$

$$Q_s = \frac{3}{2}\frac{\omega_1}{\sigma L_s}|\psi_s^r|\left(\frac{L_o}{L_r}|\psi_r^r|\cos\theta - |\psi_s^r|\right) \tag{24}$$

By derivation of Equation (23) we will have [8]:

$$\frac{dP_s}{dt} = -\frac{3}{2}\frac{L_o}{\sigma L_s L_r}\omega_1 |\psi_s^r| \frac{d\left(|\psi_r^r|\sin\theta\right)}{dt} \tag{25}$$

$$\frac{dQ_s}{dt} = \frac{3}{2}\frac{L_o}{\sigma L_s L_r}\omega_1 |\psi_s^r| \frac{d\left(|\psi_r^r|\cos\theta\right)}{dt} \tag{26}$$

Regarding to Equation (24) it seems that fast changes of active and reactive powers are obtained by changing the $|\psi_r^r|\sin\theta$ and $|\psi_r^r|\cos\theta$, respectively.

From Figure 7 it is clear that $|\psi_r^r|\sin\theta$ and $|\psi_r^r|\cos\theta$ is components of rotor flux vector, which are respectively perpendicular and conformed with stator flux vector. It shows that if rotor flux changes in direction of stator flux (change of $|\psi_r^r|\cos\theta$), reactive power Q_s changes and if rotor flux changes in vertical direction of stature flux (change of $|\psi_r^r|\sin\theta$), active power P_s changes, primary position of rotor flux and its amplitude has no effect on changes of active and reactive power. In this method eight special vectors V_0 (000) –V_7 (111) for rotor side converter is allocated the same as Figure 8.

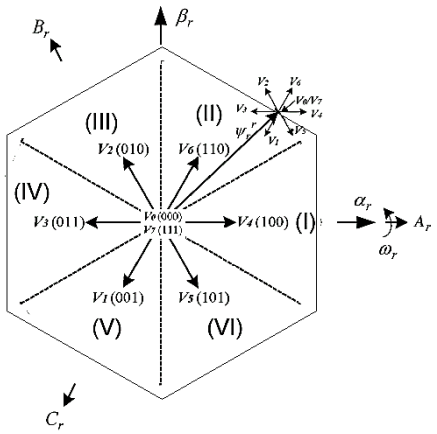

Figure 8. Voltage vectors and the control of flux using voltage vectors [8]

In considering Figure 6, the rotor flux of DFIG in reference frame of rotor is expressed as:

$$\frac{d\psi_r^r}{dt} = V_r^r - R_r I_r^r \quad (27)$$

Equation (22) shows that by neglecting rotor resistance, the rotor flux changes is determined by applied voltage to rotor, so the rotor flux moves in direction of rotor voltage and its speed changes is proportionated with domain of applied voltage vector. Thus, by choosing a proper voltage vector, movement of rotor flux can be controlled. Choosing the appropriate voltage vector is depended on position of flux linkage.

In this Process, the plate of α_r - β_r, which rotates in the speed of the rotor, is divided in six area which is shown in Figure 8. The position of eight voltage vectors is also constant to this rotating plate. Also two three-level hysteresis comparator has been used for producing the active power state (S_p) and reactive power state (S_q) the same as Figure 9.

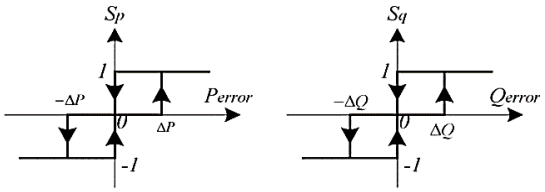

Figure 9. Active and reactive power hysteresis control [8]

The scheme of direct power control method has been shown in the Figure 10. According to Equation (24) and by using the output information of hysteresis and stator flux vector position in rotor reference frame, a switching table is presented in Table 1 which include optimized rotor voltage vectors to decrease the error of active and reactive powers from their reference values.

In this method, due to use of hysteresis controllers and absence of fixed frequency switching pattern, switching frequency is variable, which creates some problems in designing filter, moreover existence of spread harmonic spectrum and ripples in current, will have a bad impact on network. But due to lack of using any switching pattern, applying this control method is simple [8-11]. Based on this modulation methods, reaction speed in DPC is high.

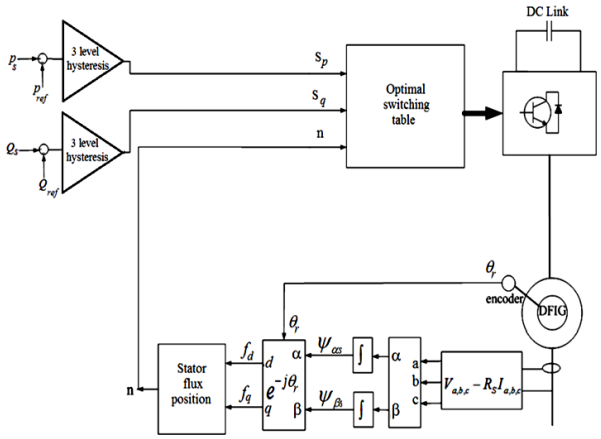

Figure 10. Schematic of the FOC implementation for rotor side converter

Table 1. Optimal switching table [8]

		I	II	III	IV	V	VI
S_q=1	S_q= 1	101	100	110	010	011	001
	S_q= 0	100	110	010	011	001	101
	S_q=-1	110	010	011	001	101	100
S_q=0	S_q= 1	001	101	100	110	010	011
	S_q= 0	111/000	111/000	111/000	111/000	111/000	111/000
	S_q=-1	010	011	001	101	100	110
S_q= -1	S_q= 1	001	101	100	110	010	011
	S_q= 0	011	001	101	100	110	010
	S_q=-1	010	011	001	101	100	110

IV. SIMULATIONS RESULTS

In this section explained control strategies in previous sections, has been simulated on a double-fed induction generator and its behavior in different condition has been surveyed. Simulation has been done by PSCAD/EMTDC and the DFIG is rated at 2 MW and its parameters has been presented in Table 2. So, as mentioned in previous sections, main consideration of this thesis is the control strategy of rotor side converter.

The network side converter control has been implemented by using of presented strategy in [5] for DC link voltage control. Simulation of rotor side converter control system, which has been explained completely, implemented by FOC and DPC methods, and their dynamical behavior in the steady state has been compared with each other, and advantages and disadvantages of FOC and DPC have been surveyed.

Table 2. Parameters of the DFIG simulated

Rated Power	2 MW
Stator voltage	690 V
Stator/rotor turns ratio	0.3
R_s	0.0108 pu
R_r	0.0121 pu (referred to the stator)
L_m	3.362 pu
$L_{\sigma s}$	0.102 pu
$L_{\sigma r}$	0.11 pu (referred to the stator)
Lumped inertia constant	0.5
Number of pole pairs	2

A. Network Side Converter Controller Simulation Results

The parameters of network side converter controller have been shown in Table 3.

Table 3. Parameters of network side converter control

Control parameters for DC-link voltage	
K_{P1}	20
T_{I1}	0.7 [s]
Control parameters for current of stator (I_q, I_d)	
K_{P2}	10
T_{I2}	0.15 [s]

The value of reference voltage for DC-link is adjusted on 1200 V and the capacity of capacitor is 1600 μF. Value of the reactance connected serially to the network side converter is 0.25 mH. For network side converter, SPWM switching strategy is used that frequency of triangular carrier signal is set on 2 kHz. Since the only objective of network side converter is control of DC-link voltage, and this is only possible by controlling the i_d component of stator current, the reference value of i_q is adjusted on zero. According to Figure 11, during the simulation, DC-link voltage is controlled on 1200 V.

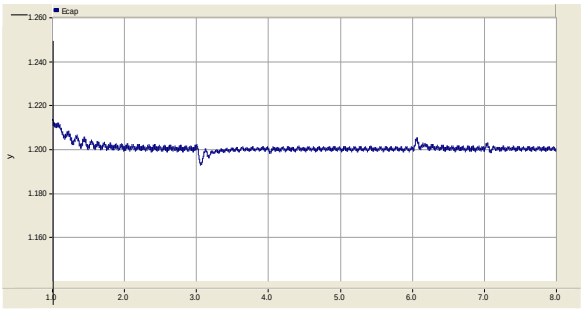

Figure 11. DC-link voltage

B. Rotor Side Converter Controller Simulation Results

At first DFIG has been supposed at speed control mode which the speed of rotor is adjusted from outside. In first step, behavior of the generator in sub-synchronous, synchronous and super-synchronous speeds has been shown by FOC and DPC methods and the effectiveness and ability of mentioned method in controlling active and reactive power of wind generator has been assessed.

Considering that flux estimation is only depended on stator resistance, in second step, control strategies performance has been surveyed by changing the stator resistance at range of 0.7 and 1.3 of its rated resistance value. In the next scenario, the DFIG is assumed in torque control mode and rotor speed, rotor current, exchanged rotor active power with network, stator active and reactive power are analyzed. The value of used parameters in FOC control strategy is provided in Table 4, also band width of hysteresis controller which has been used in DPC method, is equal to 2% of generator rated output power.

In this section generator speed has been controlled from outside and simulation results include, stator active and reactive power control , transferred active power from rotor to network and rotor current, is expressed for two control methods in synchronous and 85% and 115% of synchronous speeds. The reference of active power in second 3, has a step change from -1.8 to -0.8 MW and reactive power in second 5, has a step change from -0.6 to 0.6 MVAR.

Minus sign for active power means the injection of power to network and for reactive power means absorbing of power. Regarding to Figures 12 to 14, we can see that the strategy of direct power control the same as traditional method of Field oriented control, shows very good performance from itself in all of cases, as by choosing the hysteresis band width, the ripple of active and reactive power around the reference value can be controlled, While parameters of PI controller, presented in FOC, needs precise and complicated adjustment.

In this research, band width of three level hysteresis controller has been adjusted in 2% of generator rated power so that the ripple of active and reactive power remains in same range. Also, in considering Figure 12(a), at the moment that power reference changes, DPC method has better dynamical response (about 5 ms) comparing with FOC method (about 25 ms). As mentioned in introduction, in speed of sub-synchronous, slip is positive and rotor absorbs active power to network. During all the time of simulation, frequency of injecting current to rotor is constant and is equal with sf_s.

When rotor speed is adjusted on synchronous, slip is equal to zero and consequently rotor active power is zero and so frequency of injected current to rotor is zero (Figure 14c). In next section the value of stator resistance, applied in simulation for estimating the stator flux, have been allocated 70% and 130% of the rated value to determine the robustness of methods despite the error in stator resistance value estimation. References of active power in second 3, has a step change from -0.8 to 1.8 MW and reference of reactive power in second 5, has one step change from -0.6 to 0.6 MVAR.

As we can see in Figure 15, active and reactive power tracking is performed in both of methods. The control strategy of FOC in addition to stator resistance needs precise information of other parameters of the machine such as rotor and stator inductance and also mutual inductance; while in applying the direct power control method, the stator resistance, is needed as an input parameter, which usually is estimated.

Results show that the error caused by estimation of this parameter, do not decrease the effectiveness of this method. In next stage, the DFIG is surveyed in mode of torque control. In this step wind turbine has been used and its parameters are presented in Table 5.

Table 4. Used parameters in control strategy of FOC

Controller parameters of reactive power		Controller parameters of reactive power	
K_{P1}	1.5	K_{P2}	4
T_{I1}	0.48 [s]	T_{I2}	0.25 [s]
K_{P3}	1.5	K_{P4}	4
T_{I3}	0.48 [s]	T_{I4}	0.25 [s]

Table 5. Wind turbine parameters

rated power of wind turbine(MVA)	2 MVA
Length of wind turbine blades	40 m
air density	1.229 Kg/m3
Gear ratio	80

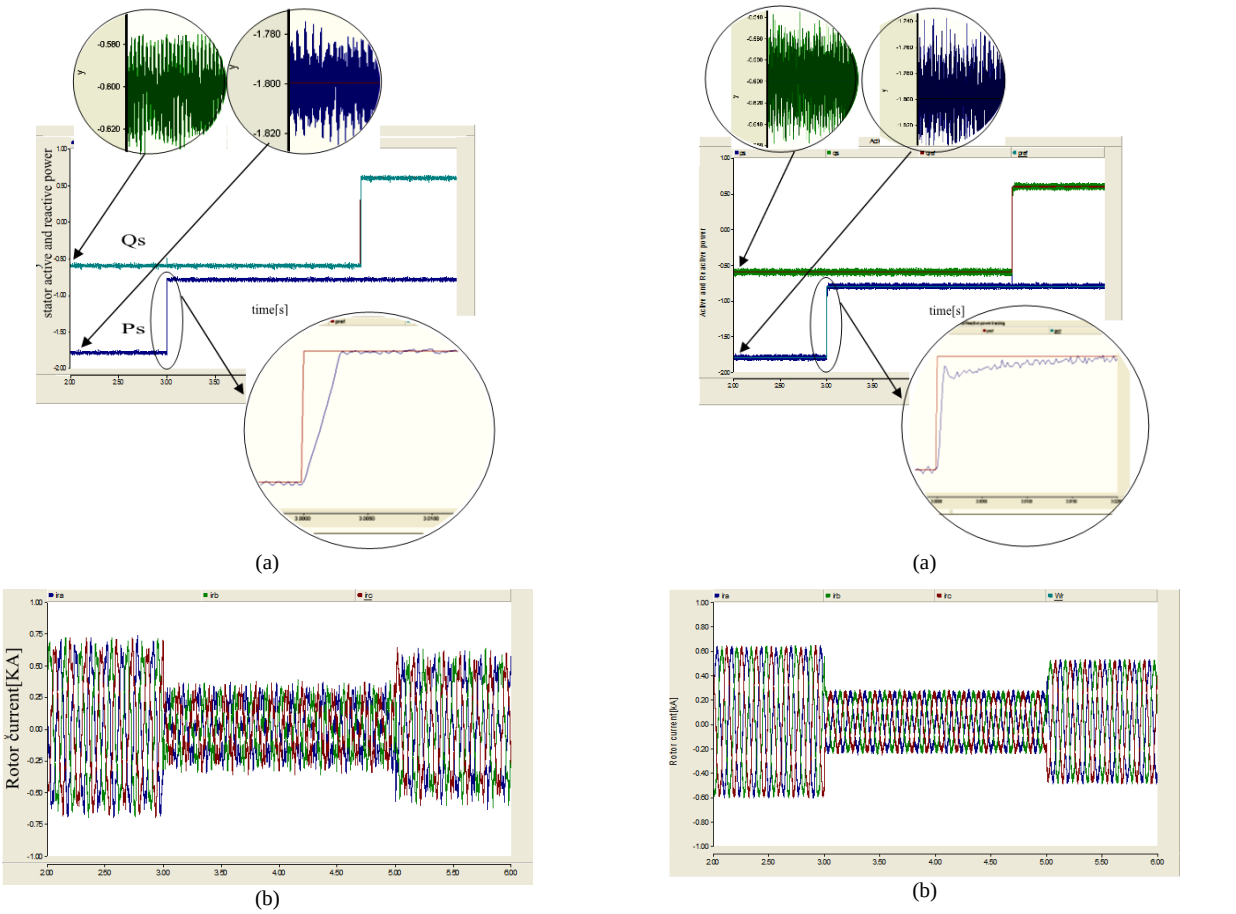

Figure 12. Simulated results under various stator active and reactive power steps and the rotor angular speed is adjusted on 0.85 pu (Sub-synchronous) (A) with DPC and (B) FOC strategy: (a) stator active power input (MW) and reactive power output (MVAR), (b) three phase rotor current (kA) (In all of figure groups the left column figures are "A" and the right column figures are "B")

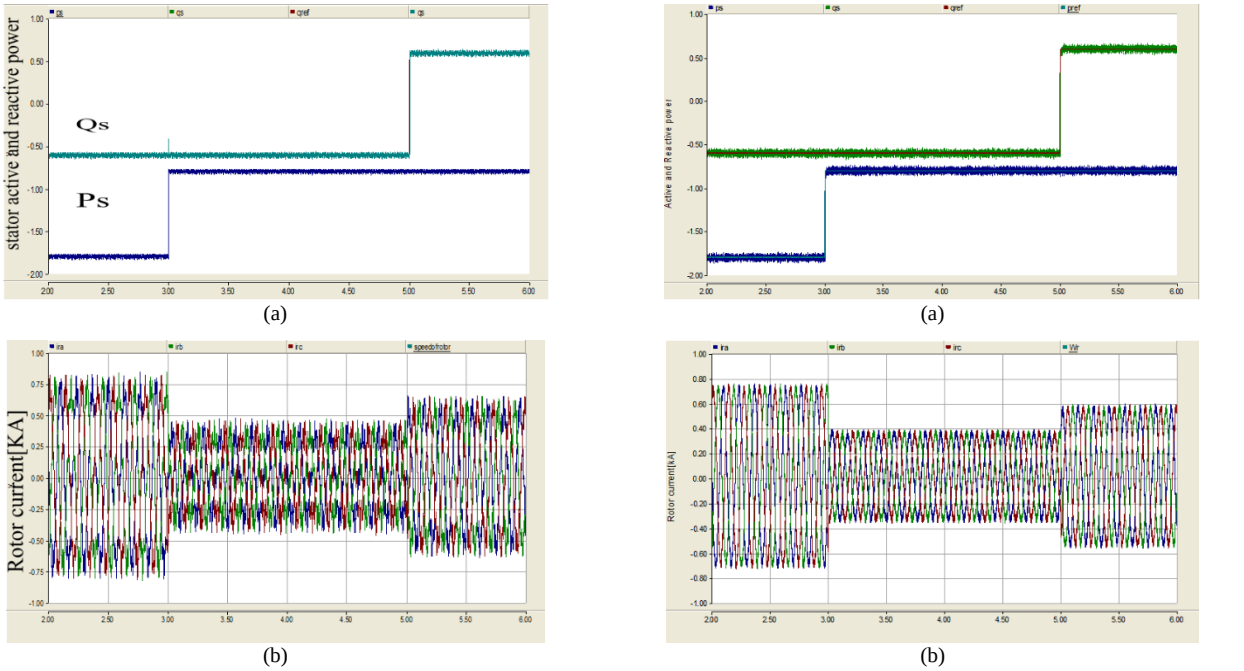

Figure 13. Simulated results under various stator active and reactive power steps and the rotor angular speed is adjusted on 1.15 pu (Super synchronous) (A) with DPC and (B) FOC strategy: (a) stator active power input (MW) and reactive power output (MVar), (b) three phase rotor current (kA)

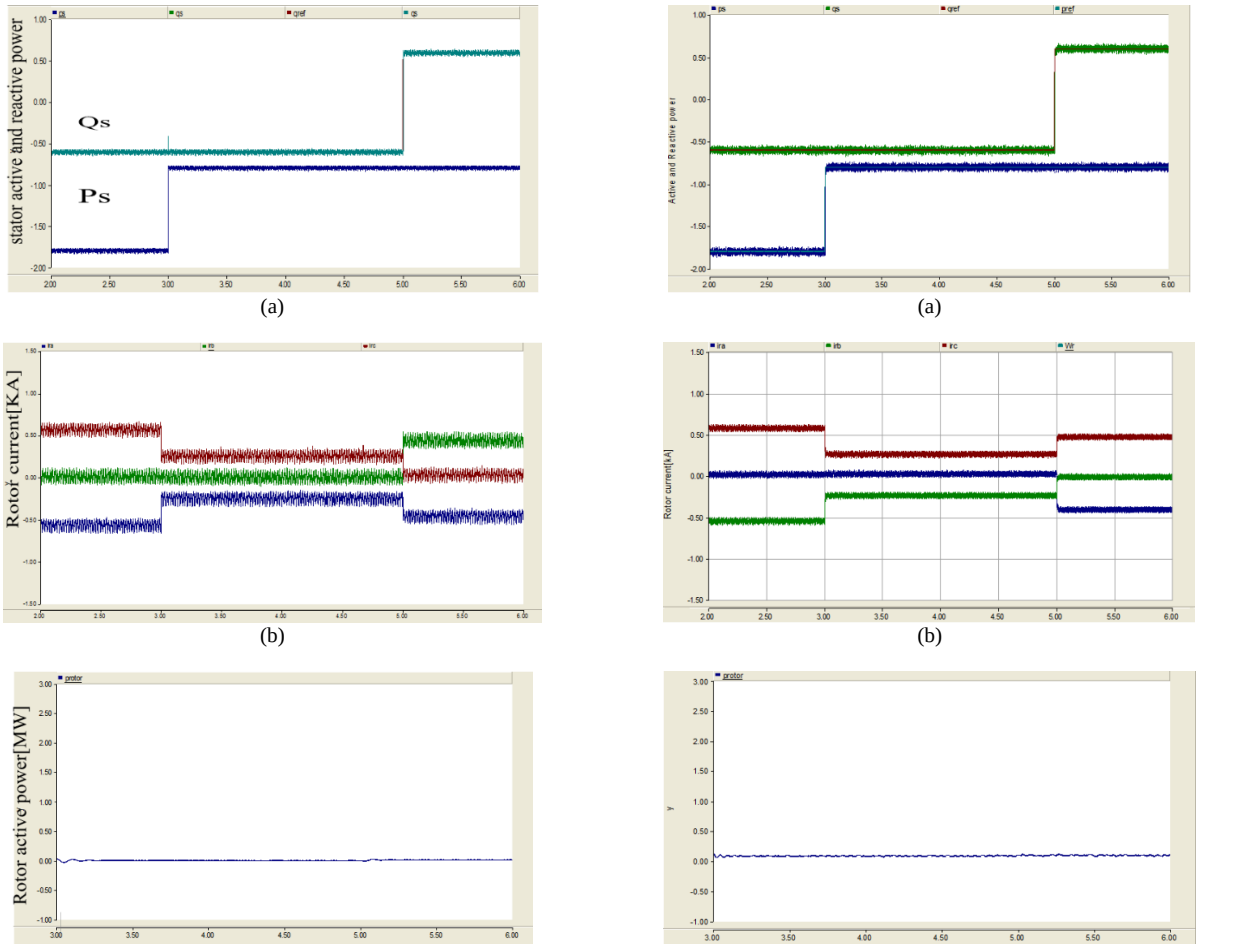

(a) (a)

(b) (b)

(c) (c)

(A) (B)

Figure 14. Simulated results under various stator active and reactive power steps and the rotor angular speed is adjusted on 1 pu (synchronous) (A) with DPC and (B) FOC strategy: (a) stator active power input (MW) and reactive power output (MVAR), (b) three phase rotor current (kA), (c) rotor active power input(MW)

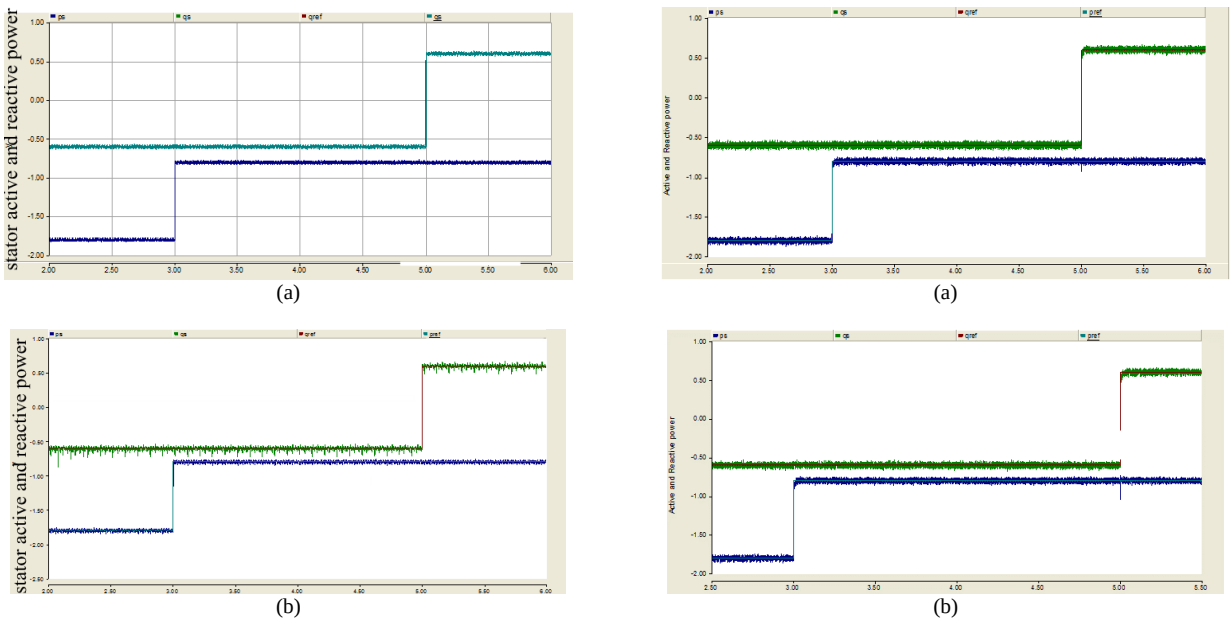

(a) (a)

(b) (b)

(A) (B)

Figure 15. Simulated results under various stator active and reactive power steps, (A) with DPC and (B) FOC strategy: (a) stator active power input (MW) and reactive power output (MVar) With 30 percent more resistance and, (b)with 30 percent less resistance than rated stator resistance

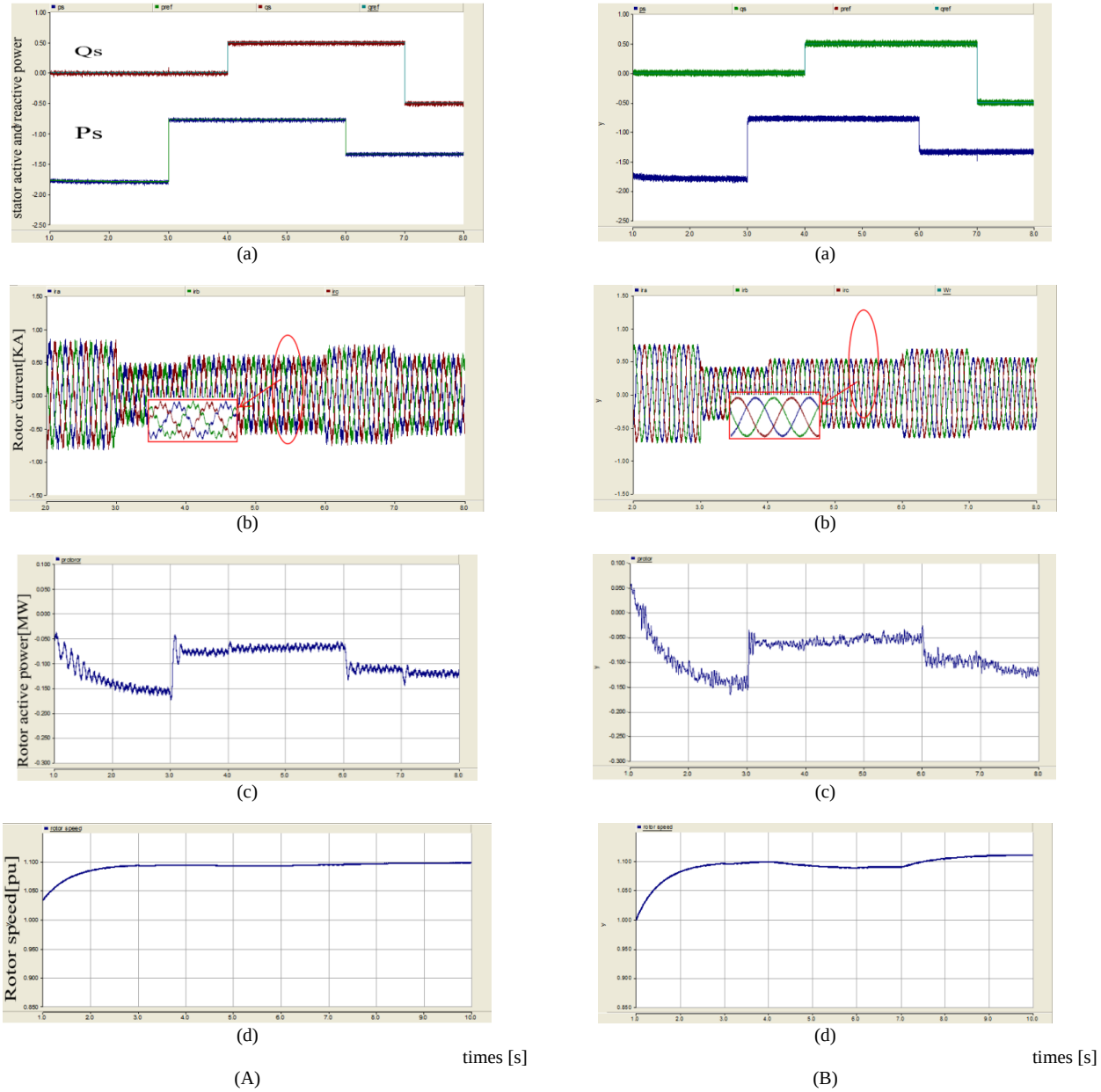

Figure 16. Simulation results with step change in mechanical input torque and under stator reactive power and active power reference adjusted to of 0.9 P_m (mechanical input power), (A) with DPC and (B) FOC strategy: (a) stator active power input (MW) and reactive power output (MVar), (b) three-phase rotor current (kA), (c) rotor active power input (MW), (d) rotor speed (pu)

In second 3, the wind velocity changes from 11.57 m/s (in this velocity turbine generates its rated power) to 9 m/s and in second 6 changes to 10.5 m/s. In the first case the stator active power reference is 0.9 of mechanical power, and in the next case it is 1.1 of output mechanical power of turbine. In this case the following results are, the stator active and reactive power exchange, the active power generated or absorbed by the rotor, the current and the speed of rotor. References of active power in second 4, has one step change from zero to 0.5 MW and in second 7 changes to -0.5 MW.

Simulation results in torque control mode, for FOC and DPC strategies are shown in Figure 16 where the active power reference equal to the 0.9 of mechanical input power. As shown in Figure 16(a) when the machine is in torque control mode, the tracking of both active and reactive power is well done in either of strategies. Moreover, according to Equation (23), since the stator active power reference equal to 0.9 of mechanical power input, the rotor injects active power into the network to balance the power. This is clearly seen in Figure 16(c). In this mode, the rotor speed is super-synchronous and Figure 16(d) illustrates this point.

$$P_m = P_s + P_r \tag{28}$$

Once more the simulation is accomplished for the case that the stator active power reference equal to 1.1 of mechanical power of the turbine. Since the stator active power reference equal to 1.1 of mechanical power input, the rotor absorbs active power from the network to balance the power. This can be seen in Figure 17(c). The rotor speed in this case is sub-synchronous.

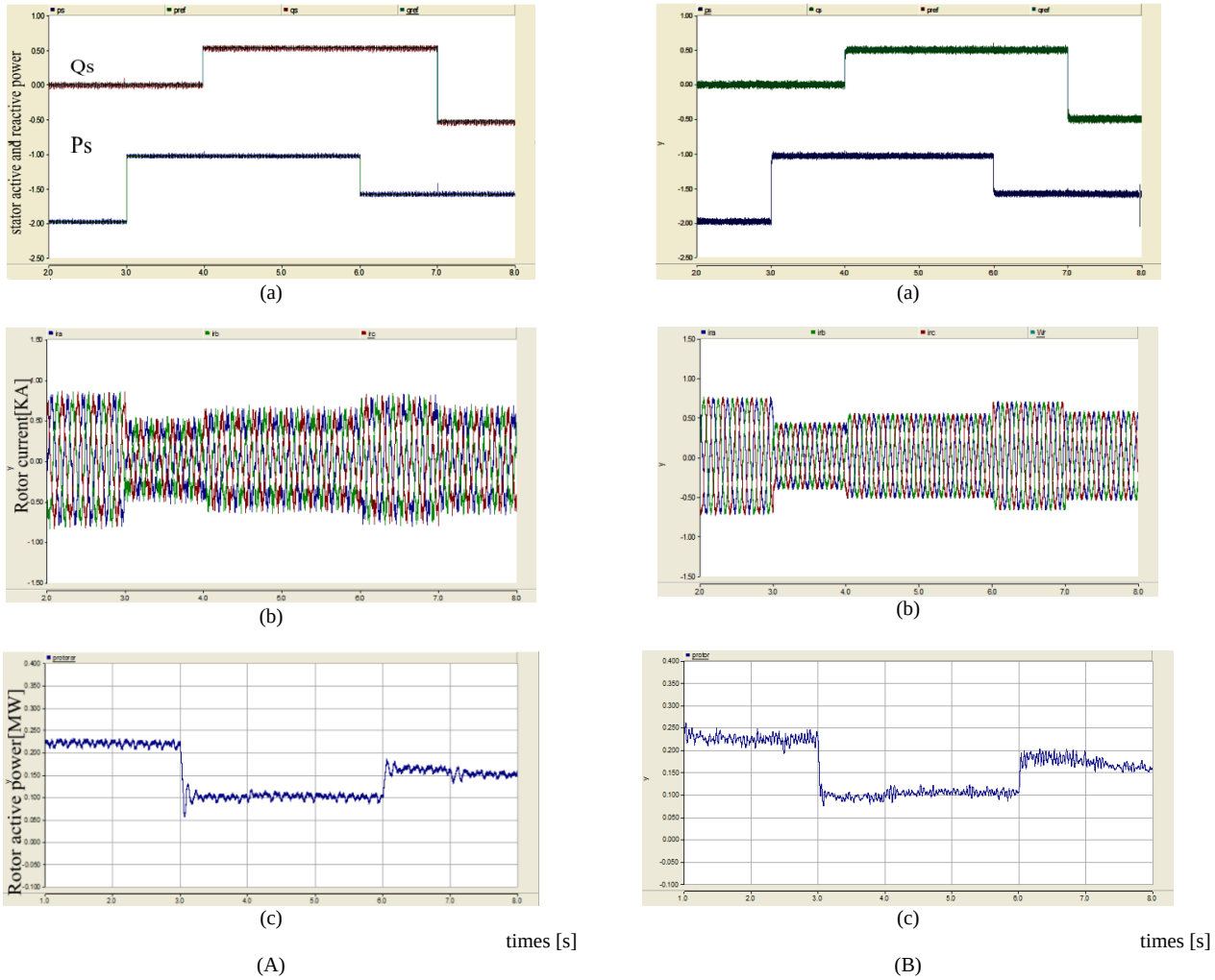

Figure 17. Simulated results with step change in mechanical input torque and under stator reactive power and active power reference adjusted to 1.1 of Pm(mechanical input power) (A) with DPC and (B) FOC strategy: (a) stator active power input (MW) and reactive power output (MVar), (b) three-phase rotor current (kA), (c) rotor active power input (MW)

V. CONCLUSIONS

In this research control of active and reactive power of a double-fed induction generator have been surveyed by using two control method based on field oriented control and direct power control and then the results have been compared with each other in different scenarios. First simulation section shows the performance of mentioned strategy in different rotor speed condition including super-synchronous, synchronous and sub-synchronous.

In the simulation results we can see that the strategy of direct power control has very good performance in various rotor speeds including super-synchronous, synchronous and sub-synchronous, the same as traditional method of field oriented control, as by choosing the hysteresis band width, the ripple of active and reactive power around the reference value can be controlled, while parameters of PI controller, presented in FOC, needs precise and complicated adjustment.

In applying the direct power control method, the stator resistance, is needed as an input parameter, which usually is estimated. In the second section the value of stator resistance, applied in simulation, have been allocated 70% and 130% of the rated value to determine the robustness of methods despite the error in stator resistance value estimation. Results show that the error caused by estimation of this parameter, do not decrease the effectiveness of this method. In the next step, double-fed induction generator in torque control mode is surveyed and obtained results show that direct power control, not only is simple, but also has faster dynamic response and good performance in different conditions.

REFERENCES

[1] M. Nunes, J. Lopes, H. Zurn, "Influence of the Variable-Speed Wind Generators in Transient Stability Margin of the Conventional Generators Integrated in Electrical Grids", IEEE Trans. Energy Conversion, Vol. 19, No. 4, pp. 692-701, Dec. 2004

[2] J.F. Manwell, J.G. McGowan, A.L. Rogers, "Wind Energy Explained - Theory, Design and Application", John Wiley & Sons, ISBN 978-0-470-01500-1, 2009.

[3] O. Anaya Lara, N. Jenkins, J. Ekanayake, P. Cartwright, M. Hughes, "Wind Energy Generation - Modeling and Control", John Wiley & Sons, ISBN 978-0-470-71433-1, New York, NY, USA, 2009.

[4] G. Abad, J. Lopez, M. A. Rodriguez, L. Marroyo, G.I. Wanski, "Doubly Fed Induction Machine: Modeling and Control for Wind Energy Generation", John Wiley & Sons, ISBN: 9781118104965, September 2011.
[5] R. Pena, J. Clare, G. Asher, "Doubly Fed Induction Generator Using Back-to-Back PWM Converters and its Application to Variable Speed Wind-Energy Generation", IEE Proc. Electric Power Application, Vol. 143, No. 3, pp. 231-241, May 1996.
[6] Y. Tang, L. Xu., "A Flexible Active and Reactive Power Control Strategy for a Variable Speed Constant Frequency Generating System", IEEE Trans. Power Electronics, Vol. 10, No. 4, pp. 472-478, July 1995.
[7] M. Yamamoto, O. Motoyoshi, "Active and Reactive Power Control for Doubly-Fed Wound Rotor Induction Generator", IEEE Trans. Power Electronic, Vol. 6, No. 4, pp. 624-629, October 1991.
[8] L. Xu, P. Cartwright, "Direct Active and Reactive Power Control of DFIG for Wind Energy Generation", IEEE Trans. Energy Conversion, Vol. 21, No. 3, pp. 750-758, September 2006.
[9] D. Santos Martin, J. Rodriguez Amenedo, S. Arnalte, "Direct Power Control Applied to Doubly Fed Induction Generator under Unbalanced Grid Voltage Conditions", IEEE Trans. Power Electronics, Vol. 23, No. 5, pp. 2328-2336, 2008.
[10] P. Zhou, Y. He, D. Sun, "Improved Direct Power Control of a DFIG Based Wind Turbine Network Unbalance", IEEE Trans. on Power Systems, Vol. 24, No. 11, pp. 2465-2474, November 2009.
[11] A.J. Sguarezi Filho, M.E. Oliveira Filho, E. Rubbert Filho, "A Predictive Power Control for Wind Energy", IEEE Trans. Sustainable Energy, Vol. 2, No. 1, pp. 97-105, January 2011.
[12] A. Nayir, E. Rosolowski, L. Jedut, "Modeling and Control of Wind Turbine and Fault", International Journal on Technical and Physical Problems of Engineering (IJTPE), Issue 9, Vol. 3, No. 4, pp. 97-101, December 2011.
[13] A. Nayir, E. Rosolowski, L. Jedut, "New Trends in Wind Energy Modeling and Wind Turbine Control", International Journal on Technical and Physical Problems of Engineering (IJTPE), Issue 4, Vol. 2, No. 3, pp. 51-59, September 2010.

BIOGRAPHIES

Mohsen Ghorbani was born in Tehran, Iran, 1987. He received the B.Sc. degree in Electrical Power Engineering from Ardabil Branch, Islamic Azad University, Ardabil, Iran in 2010 and M.Sc. degree from Science and Research Branch, Islamic Azad University, Tehran, Iran in Electrical Power Engineering in 2013. His research interests are in the area of wind energy generation, control and dynamic interaction with electrical grid.

Babak Mozafari received his M.Sc. and Ph.D. degrees from the Electrical Engineering Department of Sharif University of Technology, Tehran, Iran in 2002 and 2006. Presently he is an Assistant Professor in the Department of Electrical Engineering, Science and Research Branch, Islamic Azad University, Tehran, Iran. His research interests are in restructured power system operation and control.

Soodabeh Soleymani received the M.Sc. and Ph.D. degrees from the Electrical Engineering Department of Sharif University of Technology, Tehran, Iran in 2003 and 2007, respectively. Since 2003, she has been at Science and Research Branch, Islamic Azad University, Tehran, Iran. Her main research interests are in the areas of electric power systems protection and operation, market power monitoring, optimization and electricity market issues. She has published up to 100 research papers on the international conferences and journals.